

Goldenhar syndrome with right circumflex aortic arch, severe coarctation and vascular ring in a twin pregnancy

Elaheh Malakan Rad

Department of Pediatric Cardiology, Children's Medical Center (Pediatrics Center of Excellence), Tehran University of Medical Sciences, Tehran, Iran

ABSTRACT

Goldenhar syndrome (GS) or oculo-auriculo-vertebral dysplasia (OAVD), involves a wide variety of organ systems. Cardiovascular anomalies are among the frequent malformations. The purpose of this report is to introduce a male case of a dizygotic twin pregnancy with GS and right circumflex aortic arch (RCAA), severe coarctation, hypoplastic aortic arch, aberrant right subclavian artery, vascular ring, bilateral renal artery stenosis, and mild Dandy-Walker syndrome. The embryology of RCAA and coarctation is revisited.

Keywords: Goldenhar syndrome, right circumflex aortic arch-embryology, vascular ring-twin-coarctation

INTRODUCTION

Goldenhar syndrome (GS) or oculo-auriculo-vertebral dysplasia (OAVD), resulting from anomalous development of the first and second branchial arches, was initially reported in 1948.^[1] However, the syndrome is named after Dr. Maurice Goldenhar, a Swiss ophthalmologist who reported the constellation of signs in 1952.^[2] A broad spectrum of ocular, auricular, vertebral, cardiovascular, pulmonary, tracheoesophageal, renal, skeletal, dental, immunodeficiency and central nervous system anomalies have been reported in this syndrome.^[3] This report is about a child with GS of a dizygotic twin pregnancy with right circumflex aortic arch (RCAA), vascular ring, severe coarctation, bilateral renal artery stenosis and mild Dandy-Walker syndrome. As to the best of our knowledge, this combination has not previously reported. Using a digital three-dimensional model of embryonic aortic arches [Figure 1] and considering the morphometric characteristics of the aortic arch in this case, the embryology of RCAA associated with coarctation was revisited.

CASE REPORT

A 7-year-old boy was referred to our clinic for evaluation of cardiac murmur. He had speech disorder, hemifacialmicrosomia, bilateral epibulbar dermolipoma, bilateral preauricular tags and triangular face. His general appearance was compatible with GS [Figure 2]. His left arm and femoral pulses were very weak and a thrill was palpable in the suprasternal notch. A grade 3/6 ejection systolic murmur was heard at the upper right and left sternal borders with wide radiation to the back. Blood pressure was not elevated in either arm. Electrocardiogram was normal, but chest X-ray showed a concavity in the upper left border of cardiac silhouette.

The patient was admitted and elective cardiac catheterization was performed. The left-sided ascending aorta, was accessed through the right axillary artery and the right-sided descending aorta was entered through the left femoral artery. Complete right heart study was performed through a right femoral access and was normal. Left ventricular pressure was 150 mmHg and pressure of descending aorta was 85/63 mmHg. Ascending and descending aortograms in antero-posterior and lateral views demonstrated right tortuous circumflex aortic arch with hypoplasia of the distal segment and long-segment coarctation without any significant collateral arteries [Figure 3 and Video Clip 1]. There was a 70 mm Hg pressure gradient (PG) between left ventricle and ascending aorta and 20 mm Hg PG between the distal aortic arch and the post-coarctation segment of descending aorta.

Video available on www.annalspc.com

Access this article online

Quick Response Code:



Website:

www.annalspc.com

DOI:

10.4103/0974-2069.140857

Address for correspondence: Dr. Elaheh Malakan Rad, Department of Pediatric Cardiology, Children's Medical Center (Pediatrics Center of Excellence), Tehran University of Medical Sciences, Tehran, Iran. E-mail: erad@tums.ac.ir

Cardiac CT angiography and cardiac magnetic resonance angiography showed a vascular ring [Figure 4] produced by the retro-esophageal segment of the right aortic arch and an aberrant hypoplastic left subclavian artery arising from the area of coarctation. Vertebral artery Doppler ultrasound study excluded subclavian steal syndrome. Patient was discussed on the Congenital Cardiovascular Interventional Study Consortium in September 2013. He was referred to surgeon for reconstruction of hypoplastic aortic arch and repair of coarctation. However, the family opted to not follow the recommendation

A simple embryologic model of paired aortic arches, including third, fourth, and sixth aortic arches, was made to explain the embryologic basis of the right circumflex aortic arch [Figure 5].

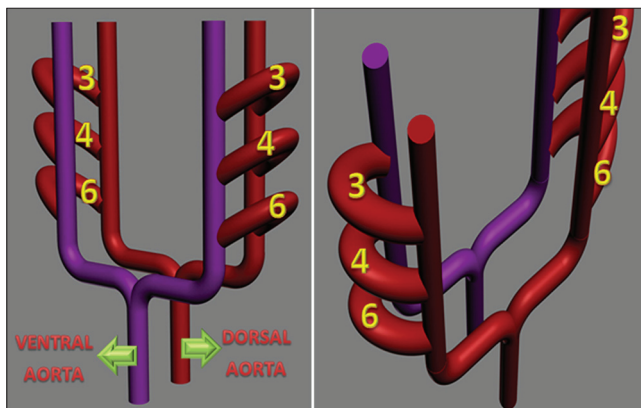


Figure 1: A digital model of the third, fourth and sixth embryonic aortic arches, made using the 3d- Max software version 2012 (Autodesk Inc.). Those parts in violet show the ventral aspect and those parts in red indicate the dorsal part

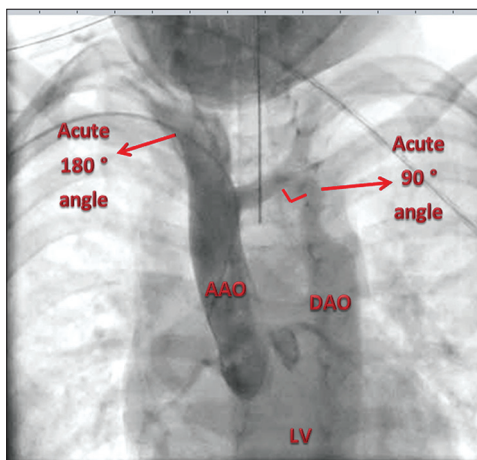


Figure 3: Ascending aortogram, accessed through right axillary artery, shows the malformed, tortuous right circumflex aortic arch. The aorta passes the right bronchus with a left-sided descending aorta. Note that the proximal part of the arch is two vertebral spaces higher than the distal aortic arch. This may mistakenly lead to the diagnosis of cervical aortic arch

Using this model and comparing the aorta of the patient with it, the embryologic basis of the development of a right aortic circumflex aortic arch was revisited.

DISCUSSION

The incidence of cardiovascular malformations in GS is reported from 5% to 58% with the tetralogy of Fallot and ventricular septal defect as the most commonly reported associated heart defects. GS occurs in about 1 in 3500 to 1:25000 live births. Sporadic, autosomal recessive and autosomal dominant cases have been reported. It has heterogeneous genetic and phenotypic features.^[3,4] Discordant involvement has been reported in twin and triplet pregnancies with only one sibling affected.^[5,6] GS occurs in infants of diabetic mothers. This anomaly has been diagnosed from intrauterine period to late adulthood. Although a variety of congenital heart disease has been reported in this syndrome but tetralogy of Fallot and ventricular septal defect are the most commonly



Figure 2: Appearance of the patient: (a) Shows hemifacial microsomia and the triangular face of the patient. (b) Indicates the bilateral epibulbar dermoid lipoma. (c) The preauricular tag of the patient

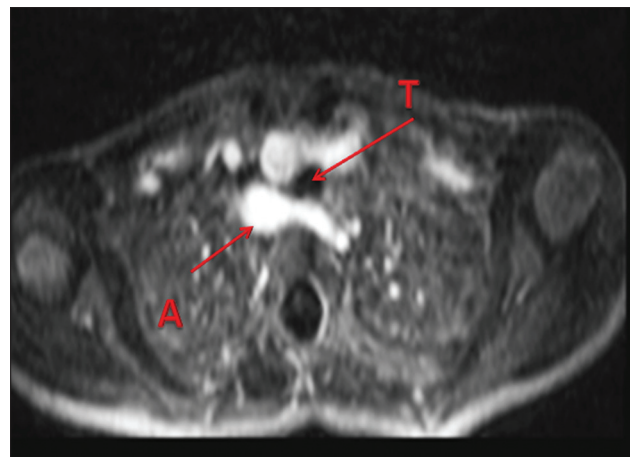


Figure 4: The vascular ring produced by the retro esophageal segment of the aortic arch (A = Aorta; T = Trachea)

cited congenital heart diseases. Coarctation and right aortic arch have repeatedly reported.^[7,8] However, as to the best of the author’s knowledge, right circumflex aorta associated with coarctation has not been reported before in GS.

We compared the morphologic characteristics of the right circumflex aortic arch with coarctation in this case with the normal right aortic arch. The parabolic morphology of a normal left aortic arch has advantages in terms of fluid mechanics.^[9] In the current case with RCAA, the length of the aortic arch is longer than normal, there are two sharp angles of approximately 180° and 90° in the proximal and distal aortic arch, respectively. The origin of left common carotid artery as the first branch of the ascending aorta, has an appearance of cactus tree [Figure 6]. The proximal aortic arch is positioned at a higher level, relative to the distal aortic arch [Figure 7]. This misleads the

clinician to an erroneous diagnosis of a cervical aortic arch. The above-mentioned morphology enables us to suggest speculation about the embryology of RCAA. Neither the difference in the level of proximal and distal aortic arch, nor the elongated length of the transverse arch is explained by the current hypothesis on embryogenesis of RCAA alone.^[10] However, both can be explained if the proximal part of the arch is thought to be derived from right third aortic arch and the distal part is derived from fourth aortic arch [Figure 8].



Figure 5: Lateral view on magnetic resonance imaging of the heart and aorta: The 180° acute angle of ascending aorta over itself, produces the characteristic “inverted v sign” on magnetic resonance imaging angiogram

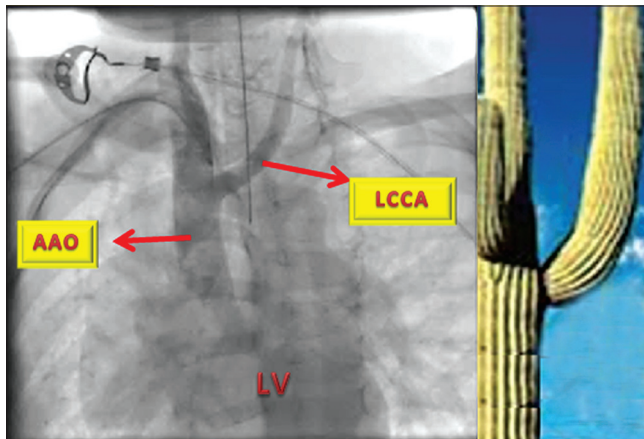


Figure 7: As in many cases of the right circumflex aortic arch, left common carotid artery (LCCA) arises as the first branch of the ascending aorta (AAO) in this case. As shown above, this particular branching produces an appearance very similar to a “cactus tree”

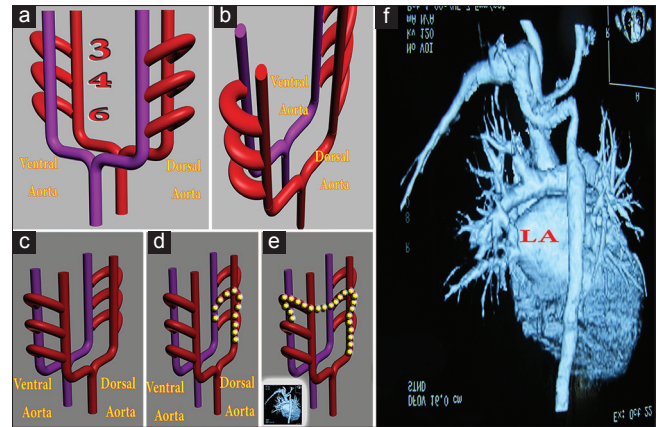


Figure 6: Embryology of the right circumflex aortic arch in this case. (a) Shows a hypothetical embryonic arch model that consists of the third, fourth and sixth aortic arches from up to down respectively. (b) The yellow small circles indicate how a normal left aortic arch is developed. (c-e) The yellow small circles demonstrate the speculation for the development of a right circumflex aortic arch. The proximal aortic arch should arise from an arch higher (i.e. the third aortic arch) than the distal aortic arch, which seems to arise from the fourth arch. This explains both the higher position of proximal arch and the elongated length of the transverse aortic arch. (f) Shows the CT angiographic image of the aortic arch in this patient

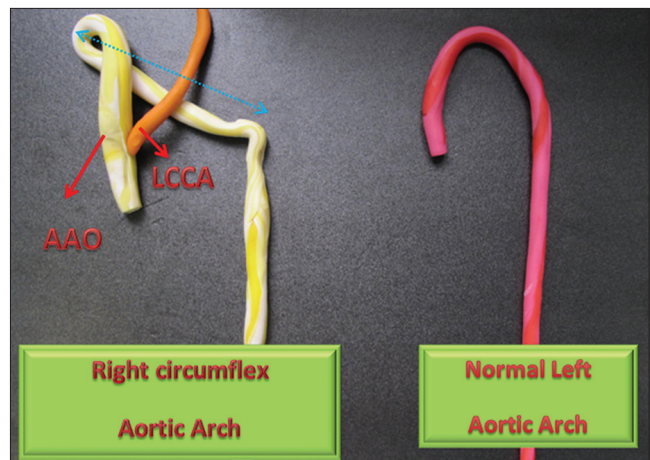


Figure 8: A schematic model of the aorta in this case with comparison to the normal left aortic arch: This figure compares the aortic arch in this case with the normal left aortic arch. Note that normally, the aortic arch has a parabolic shape. The blue arrow shows the length of the aortic arch is longer than normal in this case

ACKNOWLEDGEMENT

The author is grateful to all the colleagues on CCISC for all their invaluable comments and guidance on the reported case included in this review article. The author also deeply acknowledge the crucial technical assistance of Miss Sarah Montazmanesh, for making the digital model of embryonic aortic arches.

REFERENCES

1. Nager FR, de Reynier JP. Das gehororgan bei den angeborenen kopfmissbildungen. *Pract Otorhinolaryngol (Basel)* 1948;10:1-128.
2. Goldenhar M. Associations malformatives de l'oeillet de l'oreille, en particulier le syndrome dermoide Cpibulbaire-appendices auriculaires-fistula auriscongenita et ses Clations avec la dysostose mandibulo faciale. *J Genet Hum* 1952;1:243-82.
3. Rooryck C, Souakri N, Cailley D, Bouron J, Goizet C, Delrue MA, et al. Array-CGH analysis of a cohort of 86 patients with oculoauriculovertebral spectrum. *Am J Med Genet A* 2010;152A:1984-9.
4. Vendramini-Pittoli S, Kokitsu-Nakata NM. Oculoauriculovertebral spectrum: Report of nine familial cases with evidence of autosomal dominant inheritance and review of the literature. *Clin Dysmorphol* 2009;18:67-77.
5. Yovich JL, Stanger JD, Grauaug AA, Lunay GG, Hollingsworth P, Mulcahy MT. Fetal abnormality (Goldenhar syndrome) occurring in one of triplet infants derived from *in vitro* fertilization with possible monozygotic twinning. *J In Vitro Fert Embryo Transf* 1985;2:27-32.
6. Prasad KN, Rajha A, Vegi PK. A Case of Monozygotic Twins: The value of discordant monozygotic twins in goldenhar syndrome-OMIM%164210. *Case Rep Pediatr* 2013;2013:591350.
7. Muñoz-Pedroza LA, Arenas-Sordo ML. Clinical features of 149 patients with facio-auriculo-vertebral spectrum. *Acta Otorrinolaringol Esp* 2013;64:359-62.
8. Nakajima H, Goto G, Tanaka N, Ashiya H, Ibukiyama C. Goldenhar syndrome associated with various cardiovascular malformations. *Jpn Circ J* 1998;62:617-20.
9. Chandran KB. Flow dynamics in the human aorta: Techniques and applications. In: Leonedes CT, editor. *Biomechanical Systems: Techniques and Applications*. Boca Raton: CRC Press; 2001. p. 5.1-5.26. 30.
10. Blieden LC, Schneeweiss A, Deutsch V, Neufeld HN. Right aortic arch with left descending aorta (circumflex aorta). Roentgenographic diagnosis. *Pediatr Radiol* 1978;6:208-10.

How to cite this article: Rad EM. Goldenhar syndrome with right circumflex aortic arch, severe coarctation and vascular ring in a twin pregnancy. *Ann Pediatr Card* 2014;7:217-20.

Source of Support: Nil, **Conflict of Interest:** None declared